# Supporting Information

## Chan et al. 10.1073/pnas.0914585107

### SI Materials and Methods

**Materials.** Human collagen IV, human collagen I, and Matrigel growth factor reduced LDEV free were purchased from BD Biosciences. Soybean lecithin was purchased from Alfa Aeser. 1,2-Distearoyl-sn-Glycero-3-Phosphoethanolamine-*N*-[Maleimide (PolyethyleneGlycol) 2000] (ammonium salt) (DSPE-PEG-maleimide) and 1,2-Distearoyl-sn-Glycero-3-Phosphoethanolamine-N-[Methoxy (PolyethyleneGlycol) 2000] (ammonium salt) (DSPE-PEG) were purchased from Avanti Polar Lipids. Poly ($_{D,L}$-lactic-*co*glycolic acid) (PLGA) polymers (inherent viscosity: 0.19 dL/g) were purchased from Durect Corporation. All peptides were custom synthesized by GenScript with C-terminal amidation and purified by RP-HPLC to >95% purity by mass spectral analysis. Peptides were synthesized with a linker sequence (GGGC) at the C terminus for maleimide-thiol coupling. Alexa Fluor 647 hydrazide Tris(triethylammonium) salt was purchased from Invitrogen.

**Matrigel Binding Studies.** Ninety-six-well plates were coated with 100 μL 1/50 dilutions of Matrigel in TBS overnight at 4 °C or TBS buffer only. Plates were blocked with 3% BSA/TBS for 2 h at RT and washed three times; $10^{10}$ pfu of each phage clone was added in 0.5% TBST in triplicate to either Matrigel or BSA-coated wells. Bound phage particles were detected with peroxidase-conjugated mouse anti-M13 monoclonal antibodies (mAb) at 1/5,000 dilution (Amersham). After a 1 h incubation, the reaction was developed with 2,2′-azino-bis(3-ethylbenzthiazoline-6-sulphonic acid) (ABTS) (Amersham) and the absorbance was read at 405 nm against a reference wavelength of 490 nm with a SpectraMax Plus 384 microplate reader (Molecular Devices).

**$IC_{50}$ Value Determination of Phage Clones.** Matrigel-coated and blocked 96-well plates were incubated in triplicate with $10^{-5}$–$10^{-10}$ M peptide concentrations and $10^9$ pfu of phage in 100 μL 0.5% TBST. After 1 h at RT, bound phages were labeled with anti-M13 mAbs and color was developed and detected by ABTS absorbance (405–490 nm). Peptide inhibition curves were normalized on a percentage scale. $IC_{50}$ values were calculated using a dose–response curve fit by the formula: Y = Bottom + (Top − Bottom)/(1 + 10^[(Log$IC_{50}$ − X)*HillSlope)] (Origin 8 data analysis software).

**Release Kinetics Studies.** To assess the Ptxl–PLA bond, Ptxl and Ptxl–PLA conjugates were subject to RP-HPLC using an Agilent 1100 HPLC equipped with a pentafluorophenyl column (Curosil-PFP, 250 × 4.6 mm, 5 μm; Phenomenex). Ptxl and Ptxl–PLA absorbance was measured with an UV–Vis detector at 227 nm in a 1/1 acetonitrile/1% trifluoroacetic acid 1 mL/min nongradient mobile phase. To quantify the Ptxl–PLA drug release profile, a 2-mg nanoburr sample was divided equally into Slide-A-Lyzer MINI dialysis microtubes with a molecular weight cutoff of 20,000 Da (Pierce). The remaining Ptxl–PLA was quantified at various time points by RP-HPLC. Experiments were carried out in triplicate in PBS at 37 °C.

**Optical Imaging and Fluorescence Microscopy Studies.** Tissues were fixed in 4% paraformaldehyde/4% sucrose/saline overnight at 4 °C. Whole tissue sections were imaged simultaneously using the IVIS Imaging System 200 Series at 640/700 (ex/em) wavelength, exposure time = 1 s, binning = medium, F/Stop = 2. Tissue sections were overlayed onto photographs taken at binning = medium, F/Stop = 8. After IVIS imaging, the same tissues were OCT-frozen and cut to give approximately 10-μM sections for fluorescent microscopy. Representative H&E stained slides were made from paraffin-fixed sections. All histology sections were done by Massachusetts Institute of Technology Koch Institute Histology Facility and imaged using a DeltaVision RT deconvolution microscope using the 10× or 20× objective (Applied Precision Inc.).

**Statistical Analysis.** Student's *t* test or one-way ANOVA with post hoc Tukey tests were used to determine significance. All error bars represent the SD of the mean.

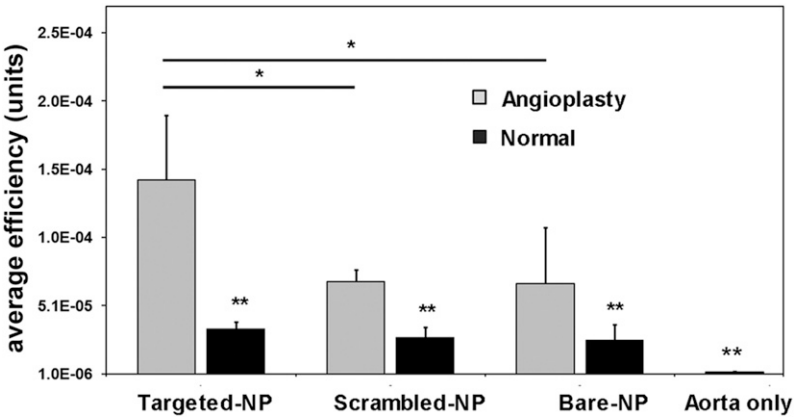


**Fig. S1.** Quantification of nanoburr binding ex vivo to angioplastied aortas. Aorta sections ($n = 3$) were analyzed using the region-of-interest (ROI) function of the IVIS Living Image Software. Values are shown here as average fluorescence efficiency (rfu) (mean ± SD). Aorta-only sections did not have nanoparticles delivered into them. *, $P < 0.05$, **, $P < 0.01$ by one-way analysis of variance with Tukey post hoc test.

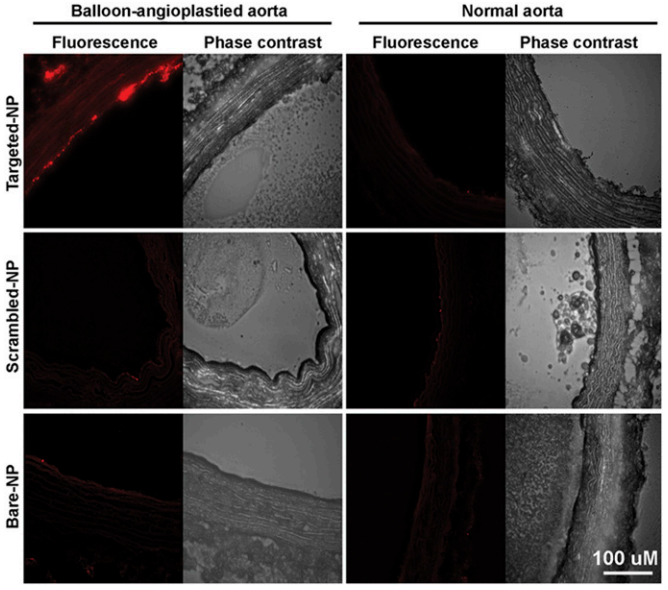


**Fig. S2.** Representative images of nanoburr binding to angioplastied and normal aortas ex vivo. (*Top*) Fluorescence and phase contrast images of aortas incubated with nanoburrs. (*Middle*) Aortas incubated with scrambled-peptide NPs. (*Bottom*) Aortas incubated with nontargeted NPs. (Scale bar, 100 μm.) Images were obtained with a DeltaVision deconvolution microscope using the 20× objective.

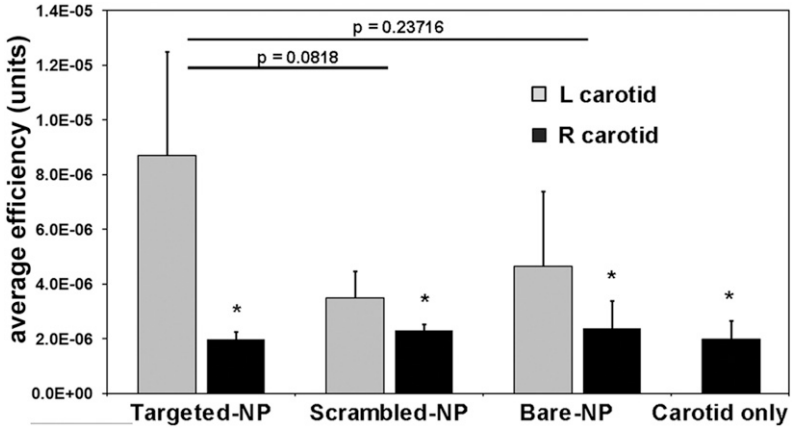


**Fig. S3.** Quantification of nanoburr binding in vivo to angioplastied left common carotids by IA delivery. Both the left and right common carotid arteries ($n = 3$) were analyzed using the ROI function of the IVIS Living Image Software. Values are shown here as average fluorescence efficiency (rfu) (mean ± SD). Carotid-only sections did not have nanoparticles delivered into them. *, $P < 0.05$ by one-way analysis of variance with Tukey post hoc test.

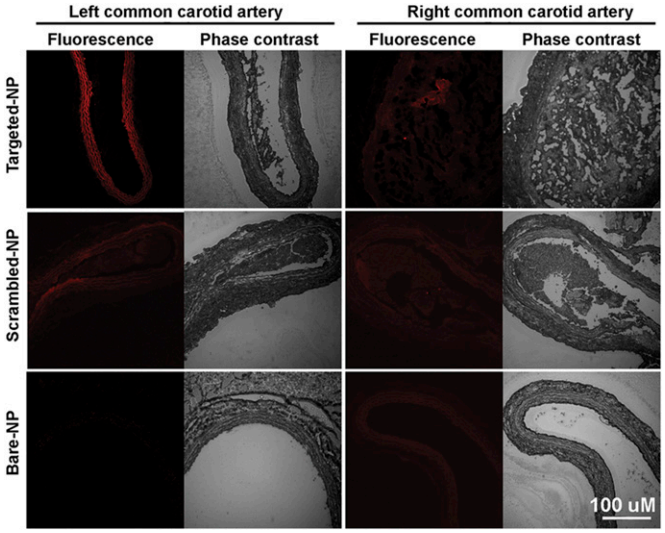


**Fig. S4.** Representative images of nanoburr binding in vivo by IA delivery to angioplastied left common carotids. (*Top*) Fluorescence and phase contrast images of carotid arteries incubated with nanoburrs. (*Middle*) Carotid arteries incubated with scrambled-peptide NPs. (*Bottom*) Carotid arteries incubated with nontargeted NPs. (Scale bar, 100 μm.) Images were obtained with a DeltaVision deconvolution microscope using the 20× objective.

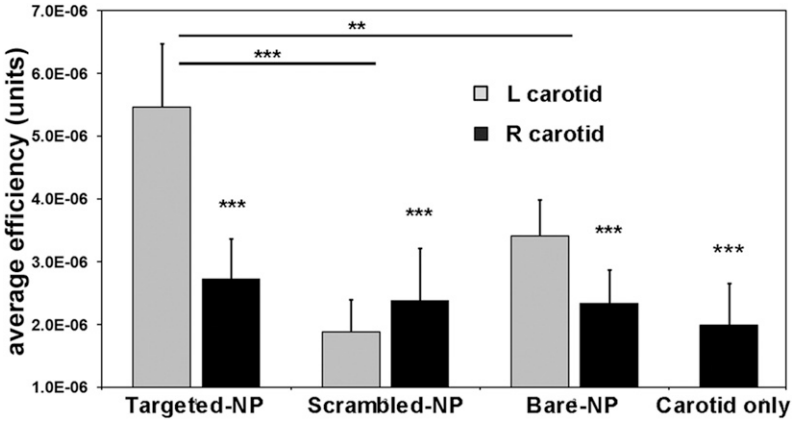


**Fig. S5.** Quantification of nanoburr binding in vivo to angioplastied left common carotids by i.v. delivery. Both the left and right common carotid arteries ($n = 5$) were analyzed using the ROI function of the IVIS Living Image Software. Values are shown here as average fluorescence efficiency (rfu) (mean ± SD). Carotid-only sections did not have nanoparticles delivered into them. **, $P < 0.01$; ***, $P < 0.001$ by one-way analysis of variance with Tukey post hoc test.

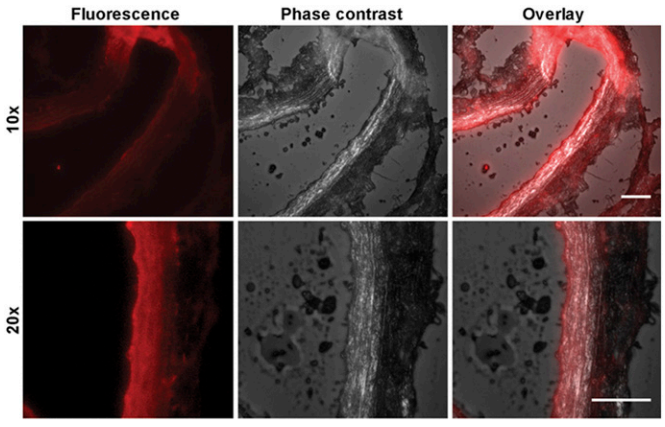


**Fig S6.** Representative images of nanoburr binding in vivo by i.v. delivery to angioplastied left common carotids. (*Left* to *Right*) fluorescence, phase contrast and overlay images of angioplastied left common carotid arteries incubated with nanoburrs at 10× and 20× magnification. (Scale bar, 100 μm.) Images were obtained with a DeltaVision deconvolution microscope using the 10× and 20× objective.